AIAA

A01-16632

AIAA-2001-0814

Laser Absorption Measurement of Atomic Oxygen in Arc-Heater Plumes

K. Komurasaki, M. Sugimine, S. Hosoda, and Y. Arakawa

University of Tokyo,
Hongo 7-3-1, Bunkyo,
Tokyo 113-0033, Japan

39th AIAA Aerospace Sciences Meeting & Exhibit
8-11 January 2001 / Reno, NV

Laser Absorption Measurement of Atomic Oxygen in Arc-Heater Plumes

Kimiya KOMURASAKI,* Masanori SUGIMINE,† Satoshi HOSODA,† and Yoshihiro ARAKAWA‡

University of Tokyo, Hongo 7-3-1, Bunkyo, Tokyo 113-0033, Japan

Abstract

Diagnostic measurements of atomic oxygen in arc-heater plumes have been conducted by using a diode-laser absorption spectroscopy technique. Number density and translational temperature of atomic oxygen were obtained from the measured absorption line profile at 777.19 nm. As a result, in an argon-oxygen mixture plume at the total enthalpy of 9.0 MJ/kg, high number density of atomic oxygen was observed, though its electronic excitation was found under-populating. In a nitrogen-oxygen mixture plume at the total enthalpy of 19.3 MJ/kg, no absorption has been measured, though in a shock layer formed in the plume, absorption was detected and density distribution has been obtained. The measured atomic oxygen density was much lower than the value expected under equilibrium conditions.

INTRODUCTION

Arc-heaters/arcjets are often used for the tests of Thermal Protection Systems, TPS for reentry vehicles. However, it is very difficult to specify the exact plume conditions because it is usually in thermo-chemical nonequilibrium. In recent researches, its thermal features are gradually clarified by means of emission spectroscopy.[1,2] The vibrational and rotational temperatures have been deduced from the line shape of molecular emissions. As for the chemical composition of the plume, unfortunately, available information is very limited so far, except by numerical computations.

Although the heat flux to TPS would vary depending on the recombination reactions on TPS surface, neither the surface catalysis nor actual degree of dissociation are known in the tests. Therefore, measurement of chemical composition of the plume will provide useful information for TPS researches. Furthermore, the information would be useful for validation of numerical codes for high-speed reacting gas flow simulation.

For the investigation of chemical composition in the plume, a quantitative and non-intrusive measurement is desired. Laser-Induced Fluorescence technique, LIF is very powerful method because it can access directly to the ground level atoms and its sensitivity is quite high.[3,4] However, it requires reference atomic density to calibrate the intensity, and is only applicable to weekly dissociated flows (<1%), otherwise, the background emission from the excited atom is too strong to get the fluorescence.

Furthermore, LIF system would be so big and expensive that it is not applicable to all the arcjet/arc-heater facilities in the world.

Diode-laser absorption spectroscopy technique enables us to non-intrusively access to the absorbing atoms and molecules even in high temperature and/or high Mach number flows.[5-8] Although the sensitivity of density detection is not so high as that of emission spectroscopy or LIF, it is applicable to dense and highly dissociated flows even though the plume is nearly optically thick.

In this research, number density of atomic oxygen in a metastable level is measured by the diode-laser absorption spectroscopy technique. The absorption line profile is traced by modulating the laser oscillation frequency around the center absorption frequency. Number density distribution can be derived from the line-of-sight absorption measurement through Abel inversion. Translational temperature of the flow can also be deduced from the broadening of absorption line.

It is relatively difficult to estimate the ground level number density from the excited level one because the first excited energy level of any atom locates far above the ground level so that the estimation is quite sensitive to the population temperature we assume.

Since the diode-laser absorption measurement system is compact and portable, one can bring it to any high-temperature testing facilities in different locations. In this study, our system is applied to the facilities located at the university of Tokyo and at the Japan Ultra-high TEmperature Material research center, JUTEM, which is located 400km west of Tokyo. A convenient beam-scan technique compatible for most of test chambers is also described herein.

* Associate Professor, Department of Advanced Energy, Member AIAA, kimiya@k.u-tokyo.ac.jp
† Graduate Student, Department of Aeronautics and Astronautics
‡ Professor, Department of Aeronautics and Astronautics, Member AIAA

MEASUREMENT THEORY

Absorption coefficient The absorption line at 777.19 nm is one of the strongest emission and

absorption lines of atomic oxygen. By measuring the absorption profile, the population density at the absorbing electronic state, which is metastable in this case, is deduced. The relationship between laser intensity I_v and absorption coefficient k_v is expressed by Beer-Lambert law as,[9]

$$\frac{dI_v}{dx} = -k_v I_v + \varepsilon_v \qquad (1)$$

Here, ε_v is emission coefficient and v is oscillation frequency of the light. Limiting the solid angle of view very small, spontaneous emission can be eliminated. Assuming axisymmetric distributions of absorption properties in a flow, the projection of absorption coefficient along the straight line at offset y is a function of the laser absorption fraction $i_v(y) = \Delta I_v(y)/I_{v_0}$ as

$$\int_{-\infty}^{+\infty} k_v(x,y)dx = 2\int_y^R \frac{k_v(r)rdr}{\sqrt{r^2 - y^2}} = -\ln(1 - i_v(y)) \quad (2)$$

The absorption coefficient distribution is obtained by Abel-inversion as

$$k_v(r) = \frac{1}{\pi}\int_r^R \left(\frac{d\ln(1-i_v)}{dy}\right)\frac{dy}{\sqrt{y^2 - r^2}} \qquad (3)$$

Since the local absorption coefficient is a sum of an absorption coefficient and a stimulated emission coefficient, the relationship between integrated absorption coefficient $K(r)$ and population density at the absorbing state n_i is given as[11,12]

$$K(r) = \int k_v dv = \frac{\lambda^2}{8\pi}\frac{g_j}{g_i}A_{ji}n_i\left[1 - \exp\left(-\frac{\Delta E_{ij}}{kT_{ex}}\right)\right] (4)$$

Here, i, j are lower and upper energy levels, A_{ij} is the Einstein's transition probability, g_i and g_j are statistical weights, E, k and T_{ex} are energy level, Boltzmann constant and electronic excitation temperature, respectively. The transition data of atomic oxygen at 777.19nm is shown in Table 1.

Table 1   Transition data of atomic oxygen

i	j	λ(nm)	E_i(cm^{-1})	E_j(cm^{-1})	g_i	g_j	A_{ji}(10^8s^{-1})
3s5S	3p5P	777.19	73768.20	86631.45	5	7	0.369

At 777.19 nm, $\Delta E_{ij}/k$ is 18,500 K. If T_{ex} $<$ $\Delta E_{ij}/k$, stimulated emission is neglected and Eq. (4) is simplified as

$$K = \frac{\lambda^2}{8\pi}\frac{g_j}{g_i}A_{ji}n_i \qquad (5)$$

Line profile   Generally, absorption line-shape is assumed as Voigt profile that contains Doppler broadening and pressure broadening. However, in the case of arcjet/arc-heater flows in a vacuum chamber, the pressure broadening becomes much smaller than the Doppler broadening.[10] If the

temperature is 5,000 K and pressure is 500 Pa, the pressure broadening is estimated three orders of magnitude smaller than the Doppler broadening. Therefore, pressure broadening is neglected.

The Stark broadening caused by random electric field of the electrons in plasma is monotonically increases with the electron density. Then it is only noticeable in the case of high electron density plasma. In our experimental conditions, the Stark broadening of 777.19nm line is estimated less than 10MHz, which is also three orders of magnitude smaller than Doppler broadening.[6]

The translational temperature of the absorbing particle T_{Tr} can be deduced from the Doppler broadening of absorption line,

$$\frac{\Delta v_{FWHM}}{2\sqrt{\ln 2}} = \frac{v}{c}\sqrt{\frac{2kT_{Tr}}{M_A}} \qquad (6)$$

where, Δv_{FWHM} is the full width at half maximum of the line profile, c is speed of light and M_A is atomic mass of absorbing particles

In local thermal equilibrium, the ground-level number density n_0 is estimated as

$$n_0 = n_i\frac{g_0}{g_i}\exp\left(\frac{E_i}{kT_{ex}}\right) \qquad (7)$$

Here, $g_0=5$.

Unfortunately, the energy level of absorbing state is 9.165 eV higher than the ground level. Therefore, estimated ground-level density might contain large errors.

EXPERIMENTAL APPARATUS

Laser system   A tunable diode laser with an external cavity (Velocity Model 6300, New Focus, Inc.) has been used as a laser source. It guarantees minimum mode hopping during the oscillation-frequency modulation. The line-width of the laser is as small as about 1 GHz. An optical isolator is used to prevent the reflected laser beam from returning into the external cavity. A Fabry-Perot etalon with an optical frequency spacing of 1.875 GHz has been used to provide reference frequency spacing during the oscillation-frequency modulation. The laser beam was introduced into a test chamber through an optical fiber. A photograph of the optical system is shown in Fig. 1.

University of Tokyo arcjet   Experiments have been conducted using an arcjet of the university of Tokyo and an arc-heater facility of JUTEM.

The arcjet developed at the university of Tokyo is schematically shown in Fig. 2. The arcjet was originally designed for the research of carbon-material degradation in space due to the impact of energetic atomic oxygen. Argon-oxygen mixture gas

2

is used as a working gas because argon gas is inert and would enhance oxygen dissociation. In those researches, oxygen has been assumed fully dissociated, and the energy (particle speed) has been estimated from the measured thrust.

Oxygen gas ports are located downstream of the cathode to prevent the cathode oxidization. The gas flow was a mixture of 6.0 SLM of argon and 1.0 SLM of oxygen, and the specific input power was 13.8 MJ/kg. Since thermal efficiency of the arcjet was 65%, the specific total enthalpy is estimated at 9.0 MJ/kg

The background pressure was kept at 160 Pa during the operation. A photograph of the arcjet plume is shown in Fig. 3. The experimental setup is shown in Fig. 4. The optical fiber output and the photo-diode sensor are mounted on a rigid rectangular flame, which can traverse in two directions inside the vacuum chamber using stepping motors. The plume has been measured at the plane 20 mm downstream of the nozzle exit.

JUTEM arc-heater   The JUTEM arc-heater was developed for material tests in very high temperature environment. Nitrogen-oxygen gas is used as a working gas for simulating the atmospheric reentry.

The schematic of JUTEM arc-heater is shown in Fig. 5. The gas flow was the mixture of 20 SLM of nitrogen and 5.0 SLM of oxygen keeping the background pressure at 33 Pa. The flow Mach number at the nozzle exit is designed at 3. The specific input power was 24.6 MJ/kg. The thermal efficiency has not been measured yet in JUTEM.

Measured Pitot pressure and local heat flux at the center of plume were 360 Pa and 570 kW/m^2, respectively. Then, total enthalpy is estimated at 19.3 MJ/kg by the heating-rate method.[13,14]

The absorption has been measured in the plume and in a shock layer generated in front of a cylinder-shape SiC TPS material. A photograph of the arc-heater plume with the TPS model is shown in Fig. 6.

The optical fiber output and photo-diode sensor are located outside of the vacuum chamber: The fiber output is mounted on the one-dimensional traverse stage on the one side of the chamber, and the photo-diode sensor is on the other side of the chamber. The transmitted laser beam is collected on the photo-diode sensor by using an off-axis parabola mirror. This setup does not require any electric nor optical fiber accesses into the vacuum chamber. The setup is shown in Fig. 7.

DATA PROCESSING

The laser oscillation frequency has been swept linearly around the absorption center frequency. The laser signal passed through the plume is recorded as a function of time and radial position, $I(y,t)$. The etalon signal is simultaneously recorded as shown in Fig. 8. It is used to convert the time based laser signal $I(y,t)$ to the frequency based one, $I(y,v)$. Absorption fraction $i_v(y)$ is calculated using the signal without absorption $I_0(y,v)$ as

$$i_v(y)=1-I(y,v)/I_0(y,v) \qquad (8)$$

Next, the set of line-of-sight absorption data $i_v(y)$ is transformed to the local absorption coefficient $\kappa(r,v)$ by Abel-inversion using Eq. (2).

Then, each absorption line profile $\kappa(v)_{r=r}$ is curve-fitted assuming a Gaussian function as,

$$\kappa(v)_{r=r}=\kappa_{max}\exp(-(v-v_0)^2/\Delta v^2) \qquad (9)$$

Then Δv and κ_{max} are determined. The relation between Δv and the full width at half maximum Δv_{FWHM} is

$$\Delta v_{FWHM} = 2\sqrt{\ln 2}\Delta v \qquad (10)$$

The integrated absorption coefficient $K(r)$ is estimated as

$$K(r) = \kappa_{max}\sqrt{\pi}\Delta v \qquad (11)$$

The local translational temperature and number density of absorbing particle are obtained by using Eqs. (4-6).

RESULTS AND DISCUSSION

Properties in an argon-oxygen plume In the argon-oxygen plume, strong absorption up to 50 % was observed. The absorption line profile reconstructed by Abel inversion is shown in Fig. 9. The fitting error to a Gaussian curve was less than 1 %.

The radial distributions of the metastable-level number density of atomic oxygen and the translational temperature in the plume are plotted in Fig. 10. Maximum number density and temperature were 7.2E17 m^{-3} and 9,200 K, respectively.

The Boltzmann plot is shown in Fig. 11. The estimated ground-level density in thermal equilibrium case is two orders of magnitude higher than the value expected in fully dissociated case. That is, the electronic excitation of atomic oxygen is under-populating as illustrated in the figure. The population temperature of the metastable level T_{pop} should be $\geq 17,400$K

Generally, expansion flow in the nozzle is expected chemically frozen. In addition, radiative transition from the metastable level to the ground level does not occur, and collisional transition is seldom in the expanding flow. Therefore, T_{pop} would be preserved through the expansion from the constrictor.

The energy exchange rate between the electric

excitation mode and the electron translational mode is so high in the constrictor that one can expect $T_e \approx T_{pop}$ in the constrictor. (T_e is the electron temperature.).

Properties in a nitrogen-oxygen plume

In a nitrogen-oxygen plume of JUTEM arc-heater, no absorption has been observed.

The obvious difference in absorption fraction between the nitrogen-oxygen and argon-oxygen plumes implies that their thermo-chemical conditions would be quite different from each other.

As discussed in the previous section, T_{pop} and degree of dissociation in the constrictor are thought preserved through the nozzle expansion. Since metastable-level density in the plume was found under the sensitivity limit of about $1E+16 m^{-3}$, the possible combination of T_e and oxygen degree of dissociation in the constrictor is limited as shown in Fig. 12. (Isentropic expansion from the constrictor conditions; $T_{Tr} = 5,000$ K and $M = 1$ to the plume condition; $P = 33$ Pa and $M = 3$ was assumed.)

The degree of dissociation would be smaller and/or the electron temperature would be lower than in the argon-oxygen plume.

Heating processes in the constrictor

The most distinctive difference between nitrogen and argon is the elastic momentum transfer cross section of electrons. Nitrogen cross section is one order of magnitude larger than argon cross section. Then, in the nitrogen-oxygen flow, ohmic heating becomes slower and the energy transfer from electrons to heavy particles becomes faster, resulting in lower electron temperature than in the argon-oxygen flow.

However, it brings considerable decrease in electron thermal conductivity in the nitrogen-oxygen flow. As a result, high temperature region is quite localized near the cathode tip where electric current is concentrated. Then, it can happen that only the gas flowing near the cathode tip is heated up, while the gas flowing near the anode remains relatively cold.

Unfortunately, many of arc-heaters operating with oxygen mixture gas are designed to prevent the oxygen molecules from coming near the cathode for the purpose of cathode protection. Therefore, the oxygen molecules might not experience high temperatures, resulting in low degree of dissociation.

Detailed analysis on the constrictor flow will clarify those inhomogeneous heating processes.

Properties in a nitrogen-oxygen shock layer

When a cylindrical TPS model of 40 mm in diameter was inserted in the flow, a bow-shock was generated in front of the model. The probe laser of 2 mm in diameter was scanned in the middle of the shock

layer of 5 mm thick.

Figure 13 shows absorption fraction as a function of laser oscillation-frequency. Maximum absorption fraction was 0.03. The temperature deduced from the Doppler broadening is 24,700 K, which is thought much higher than the actual translational temperature because the line profile is swelled due to the flow components tangential to the TPS surface in the shock layer.

The distribution of metastable-level number density in the shock layer is shown in Fig. 14. The maximum density was $2.3E16 m^{-3}$.

Thermo-chemical equilibrium condition

The computed equilibrium chemical composition and temperature T_{eq} are listed in Table 2. An 11-species air-reaction model[15,16] is used. T_{eq} stays at around 5,000 K in this range of enthalpy due to the nitrogen dissociation.

If the shock layer is in thermo-chemical equilibrium, computed metastable-level density becomes as small as $1.5E12 m^{-3}$, which is much lower than the sensitivity limit. Therefore, the equilibrium condition cannot be expected in the shock layer.

Table 2 Computed equilibrium chemical composition and temperature. Pressure 360 Pa, enthalpy 19.3 MJ/kg

N_2 (m^{-3})	0.1833E+22
O_2 (m^{-3})	0.2535E+17
N (m^{-3})	0.1982E+22
O (m^{-3})	0.1409E+22
NO (m^{-3})	0.3171E+19
N_2+ (m^{-3})	0.2315E+16
O_2+ (m^{-3})	0.2989E+14
NO+ (m^{-3})	0.8606E+18
N+ (m^{-3})	0.2299E+17
O+ (m^{-3})	0.2502E+17
electron (m^{-3})	0.6596E+18
T_{eq} (K)	4989

Error analysis The laser signal I_v is recorded as 12-bit digital data. Then it may contain about 0.1% error of its full-scale intensity I_0. The resulting error arising in Eq. (2) is estimated as

$$\left(\frac{\Delta \ln(1 - i_v(y))}{\ln(1 - i_v(y))} \right)^2 = \left(\frac{\Delta \ln(I_v / I_{v0})}{\ln(I_v / I_{v0})} \right)^2$$
$$\approx \left(\frac{1}{(I_v / I_{v0})\ln(I_v / I_{v0})} \right)^2 2\left(\frac{\Delta I_v}{I_0} \right)^2 \qquad (12)$$

The error is plotted as a function of absorption fraction in Fig. 15. The error induced in the density profile would be 0.4 % at the 50 % absorption, while it becomes 5 % at the 3 % absorption. The error

induced in temperature estimation would be twice of those.

Since number of measurement points in the y direction is limited to 15~40, the high order variations in density profiles are lost through Abel inversion and curve-fittings. However, the average density or the density integrated though the line-of-sight is preserved.

SUMMARY

Number density and translational temperature of the atomic oxygen were deduced from the measured absorption line-shape at 777.19 nm by using a diode-laser absorption spectroscopy technique.

As a result, in the argon-oxygen mixture plume at the enthalpy of 9.0 MJ/kg, high oxygen dissociation has been observed, though its electronic excitation was found under-populating.

In a nitrogen-oxygen plume at the enthalpy of 19.3 MJ/kg, no absorption was observed. This might be due to the inhomogeneous heating inside the arc-heater.

REFERENCES

1) Tahara, H., et al.: DC Arcjet Plasma characteristics using ammonia and mixture of nitrogen and hydrogen, AIAA paper 99-3736, July, 1999.

2) Winter, M. W. and Auweter-Kurtz, M.: Boundary layer investigation in front of a blunt body in a subsonic air plasma flow by emission spectroscopic means, AIAA paper 98-2460, June, 1998.

3) Storm, P. V. and Cappelli, M. A.: Laser-induced fluorescence measurements within an arcjet thruser nozzle, AIAA paper 95-2381, July 1995.

4) Feigl, M., Dennis, J. E., Fasoulas, S. and Auweter-Kurtz, M.: Comparison of LIF and solid electrolyte sensor measurements of atomic and molecular oxygen in a plasma jet, AIAA paper 2000-0198, January 2000.

5) Arroyo, M. P., Langlogis, S. and Hanson, R. K.: Diode-laser absorption technique for simultaneous measurement of multiple gasdynamic parameters in high-speed flows containing water vapor, App. Opt., Vol. 33 (1994), pp.3296-3370.

6) Bear, D. S., Chang, H. A. and Hanson, R. K.: Semiconductor laser absorption diagnostics of atomic oxygen for atmospheric-pressure plasmas, AIAA paper 98-0822, 1998.

7) Grossmann, B. E. and Browell, E. V.: Spectroscopy of water vapor in the 720nm wavelength region: linestrangths, self-induced pressure broadenings and shifts, and temperature dependence of linewidths and shift, J. Mol. Spectroscopy, Vol. 136 (1989), pp. 264-294.

8) Zhang, F. Y., Komurasaki, K., Iida, T. and Fujiwara, T.: Diagnostics of an argon arcjet plume using a diode laser, App. Opt., Vol. 38, No. 9 (1999), pp. 1814-1822.

9) Mellon, M. G.: Analytical absorption spectroscopy (absrptimetry and colorimetry), John Willey &Sons, Inc., New York, pp. 78-98.

10) Zhang, F. Y., et al.: Simultaneous Measurements of Plume Temperature and Atomic Number Density with Optical Absorption Tomography, Proceedings of 26th IEPC, Kitakushu, Japan, 1999, pp. 278-287.

11) Zel'dovich, Y. B., Raizer, Y. P., Hayes, W. D. And Probstain, R. F.: Physics of shock waves and high-temperature hydrodynamic phenomena, Academic Press New York (1966), pp. 107-172.

12) Lochte-Holtgreven W.: Plasma Diagnostics, Norty-Holland Publishing Company, Amsterdam (1968), pp. 9-65.

13) Pope, R. B.: Measurements of Enthalpy in Low-Density Arc-Heated Flows, AIAA Journal, Vol. 6, No. 1, 1968, pp.103-110.

14) Boison, J. C. and Curtiss, H.A.: An experimental investigation of blunt body stagnation point velocity gradient, ARS Journal, 1959, pp130-135.

15) Bottin, B., Abeele, D.V., Carbonaro, M., Degrez. G. and Sarma, G.S.R.: Thermodynamic and transport properties for inductive plasma modeling, J. Thermophysics and Heat transfer, Vol. 13, No. 3, 1999.

16) Gupta, R. N., Yos, J. M., Thompson, R. A. and Lee, P. K.: A review of reaction rates and Thermodynamic and transport properties for an 11-Species air model for chemical and thermal noneqilibrium calculations to 30,000 K, NASA RP 1232, 1990.
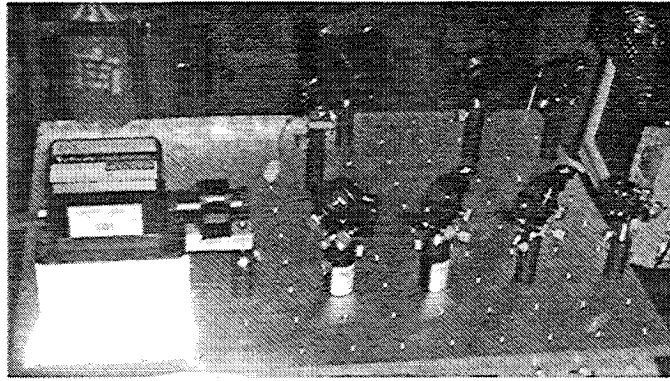
Fig. 1 Optical setup consisting of a diode-laser with an external cavity, optical isolator, Fabry Perot etalon, photo-diode, and optical-fiber input
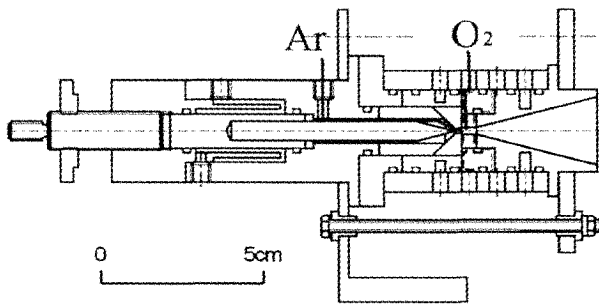
Fig.2 University of Tokyo arcjet
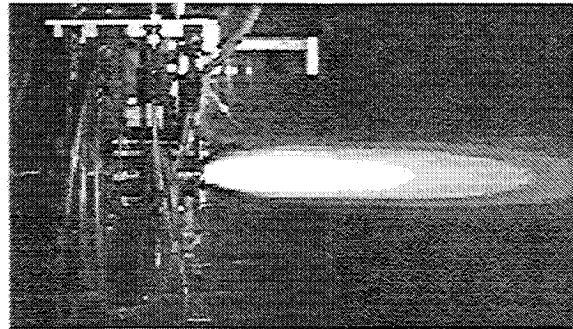
Fig. 3 Arcjet plume
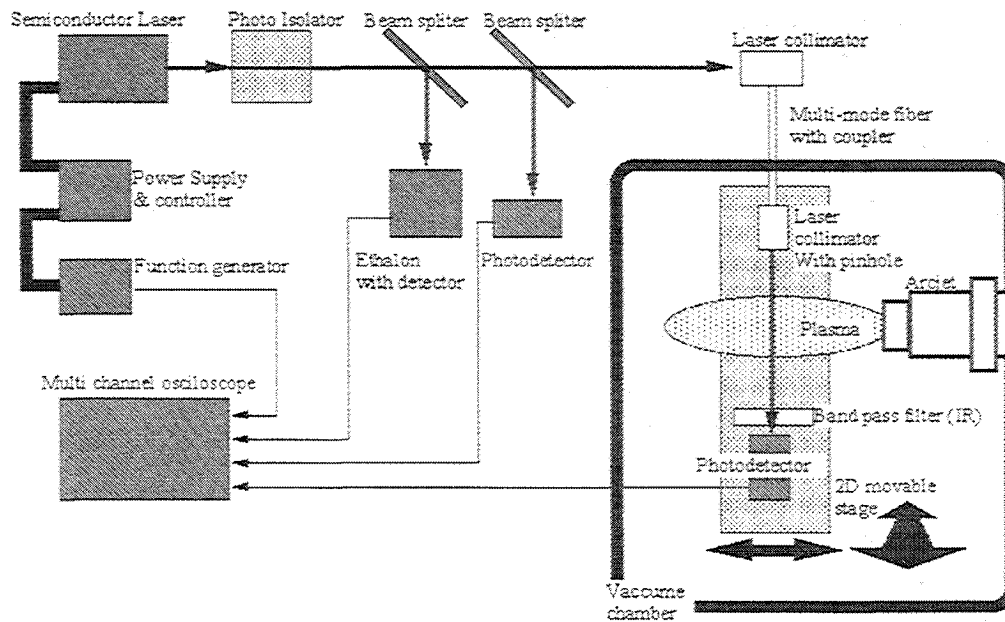
Fig. 4 Schematic of the measurement system for arcjet diagnosis at the university of Tokyo

American Institute of Aeronautics and Astronautics
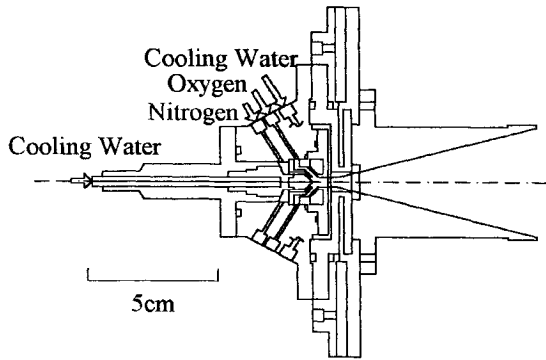
Fig. 5 JUTEM arc-heater
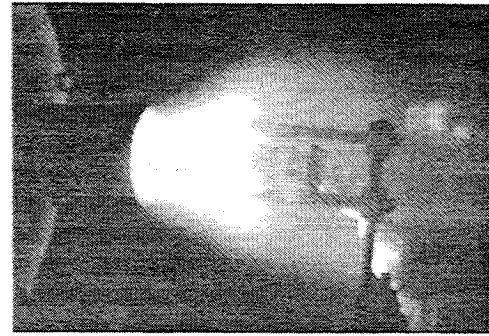
Fig. 6 Arc-heater plume with a TPS model
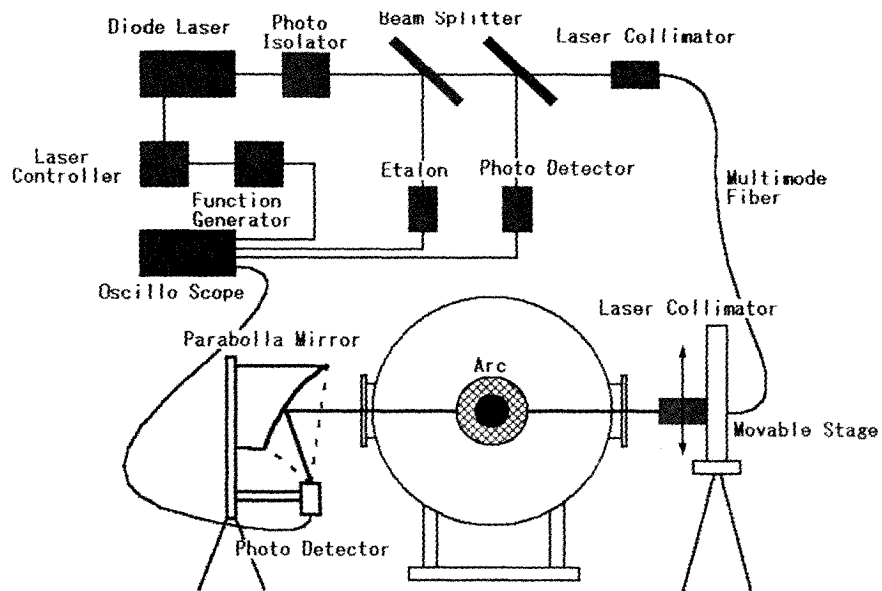
Fig. 7 Schematic of the measurement system for arc-heater diagnosis at JUTEM
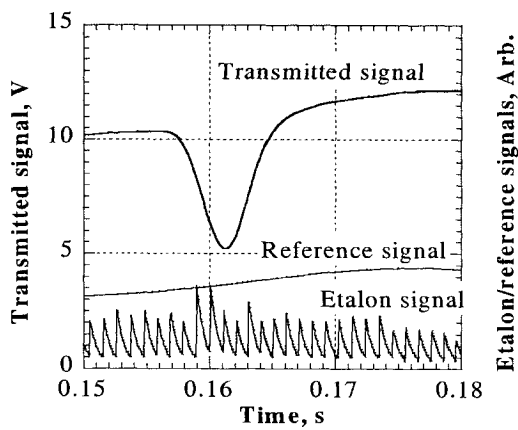
Fig. 8 Typical signals recorded
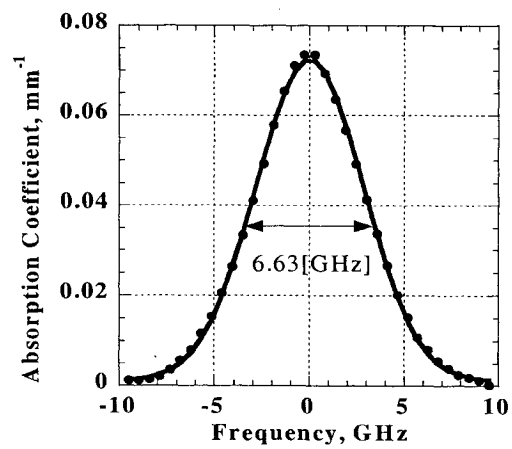
Fig. 9 Absorption line profile at the center of argon-oxygen arcjet plume

7
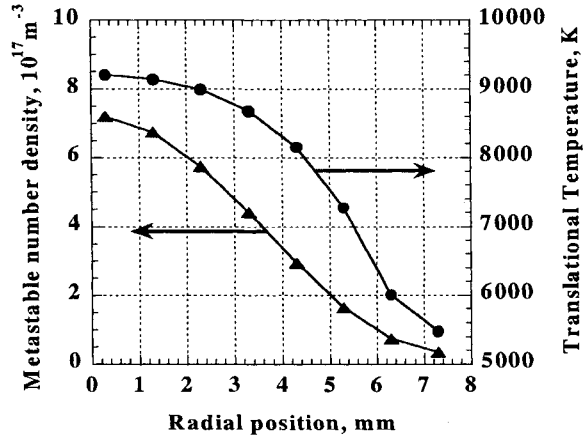
Fig. 10 Radial distributions of the atomic oxygen number density at the metastable level and the translational temperature in the plume
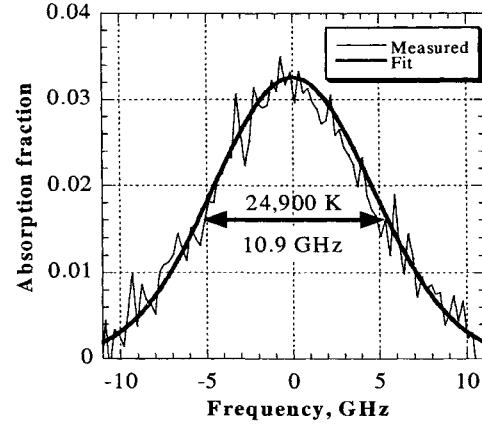
Fig. 13 Measured absorption line profile at $y=0$ in the shock layer in the JUTEM arc-heater plume
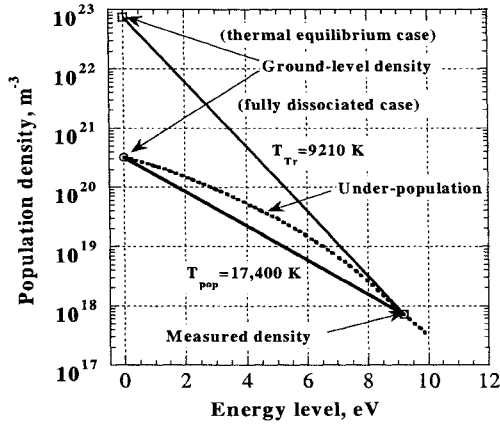
Fig. 11 Boltzmann Plot at the center of the argon-oxygen plume. Measured metastable density and estimated ground-level densities of atomic oxygen are plotted.
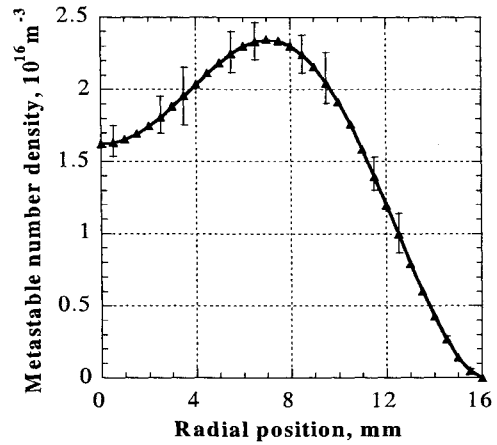
Fig. 14 Radial distribution of atomic oxygen number density at the metastable-level in the shock layer
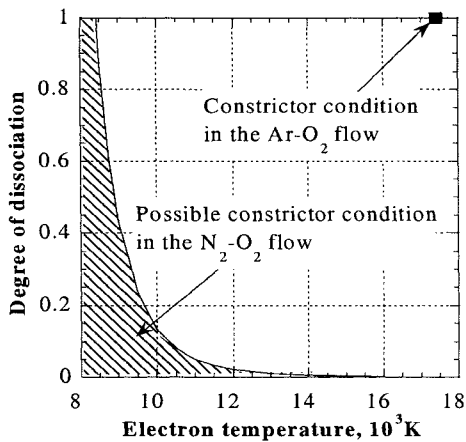
Fig. 12 Possible combination of T_e and oxygen degree of dissociation in the constrictor
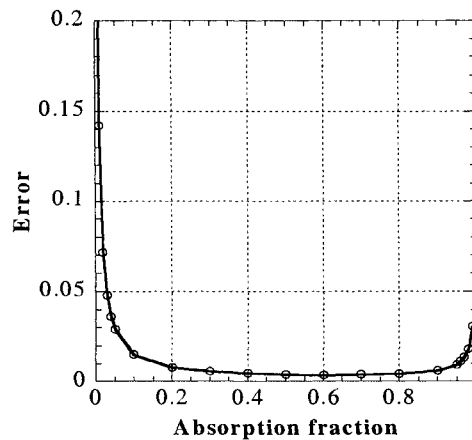
Fig. 15 Errors induced in density

8
American Institute of Aeronautics and Astronautics